COMMUNICATION

Is the surface of Hofmann-like spin-crossover {Fe(pz)[Pt(CN)₄]} the same as its bulk?

Alejandro Martínez Serra, [ID] [a] Archit Dhingra, [ID] *[a] María Carmen Asensio, [b,c] José Antonio Real [ID] [d] and Juan Francisco Sánchez Royo [ID] *[a,c]

Temperature dependent X-ray photoemission spectroscopy (XPS) has been employed to examine the spin-crossover (SCO) transition in the nanocrystals of 3D Hoffman-like {Fe(pz)[Pt(CN)₄]}. Consistent with the existing literature, the temperature-dependent variations in the Fe 2p core-level spectrum provide unambiguous evidence of the spin-state transition in this SCO complex. One of the many possible reasons behind a lack of discernible temperature-driven shifts in the binding energies of both the N 1s core-level components could be the immunity of its HS electronic configuration to thermal fluctuations. The high-spin fraction *versus* temperature plot, extrapolated from the XPS measurements, reveals that the surface of the nanocrystals of {Fe(pz)[Pt(CN)₄]} is in the high-spin state at room temperature, rendering it promising for room-temperature spintronics and quantum information science applications.

Introduction

Fe-based spin crossover (SCO) complexes, with Fe in the +2 oxidation state, are materials where the Fe(II) atoms are surrounded by an octahedral ligand field. In these Fe(II) SCO complexes, even some minor external perturbations, like variations in the magnetic field[1,2] or temperature,[3–6] can lead to a detectable change in their spin state.[7–13] Owing to the temperature sensitivity of the octahedral ligand field splitting (Δ_{oct}) between the t_{2g} and e_g orbitals, these complexes tend to occupy the low-spin state (LS), exhibiting a diamagnetic character ($S = 0$), at low temperatures. Conversely, lowering the Δ_{oct} between the t_{2g} and e_g orbitals by increasing the temperature,

beyond their respective critical transition temperature T_c, makes these complexes transition to a paramagnetic high-spin state (HS) with $S = 2$.[12,14–18] The bistability of these spin states[7,19,20] and the facility with which these spin states can be transitioned in the Fe(II) SCO complexes[6] make these materials come off as great candidates for nonvolatile memory applications.[21–23] The existence of room-temperature magnetic moment in these molecules may also be exploited for room-temperature spintronics[24,25] and molecular transistor-based quantum information science applications.[26,27] To elaborate further, as can be reasonably extrapolated from Bhatti *et al.*,[28] the bistability of the Fe(II) SCO complexes at room temperature can be capitalised upon for spintronics-based memory, and as far as room-temperature quantum information science applications are concerned, such materials can be used for the fabrication of scalable molecular transistors (described in great enough detail in ref. 27).

Usually, investigation of spin-state transitions in the SCO complexes involves the use of magnetometry (or magnetic susceptibility measurements). However, since Fe(II) experiences a considerable electronic change with a spin-state transition[29] (Fig. 1a), some popular non-invasive techniques like X-ray absorption spectroscopy and X-ray photoemission spectroscopy (XPS) have been employed to detect these transitions in the Fe(II) SCO complexes without the application of an external magnetic field.[6,30–41] In this work, temperature-dependent XPS has been used to monitor the evolution of the Fe 2p and N 1s core-level photoemission spectra of the nanocrystals of 3D Hoffman-like {Fe(pz)[Pt(CN)₄]} (schematic shown in Fig. 1b) with temperature. Besides, the highly surface-sensitive nature of XPS[42,43] would allow us to uncover the effects of thermal fluctuations on the surface magnetization of the {Fe(pz)[Pt(CN)₄]} nanocrystals, which may not be all the same when compared to the magnetization values in the bulk. Hence, the physical insights provided by these measurements could be of high relevance for nanoparticles of Fe(II) SCO complexes with high surface-to-volume ratios.[10,44,45] Also, for a reliable fabrication of nanodevices based on {Fe(pz)[Pt(CN)₄]}, the knowledge of the surface of {Fe(pz)[Pt(CN)₄]} nanocrystals

aInstitut de Ciència dels Materials de la Universitat de València (ICMUV), University of Valencia, Carrer del Catedrátic José Beltrán Martinez, 2, 46980 Paterna, Valencia, Spain. E-mail: archit.dhingra@uv.es, juan.f.sanchez@uv.es

bMaterials Science Institute of Madrid (ICMM/CSIC), Cantoblanco, E-28049 Madrid, Spain

cMATINÉE, the CSIC Associated Unit between the Materials Science Institute (ICMUV) and the ICMM, Cantoblanco, E-28049 Madrid, Spain

dInstitut de Ciència Molecular (ICMol), University of Valencia, Carrer del Catedrátic José Beltrán Martinez, 2, 46980 Paterna, Valencia, Spain
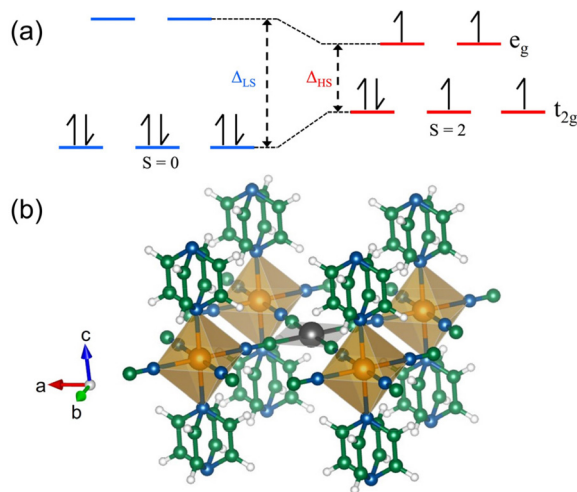
Fig. 1 (a) [Ar]$3d^6$ electronic configuration in an octahedral ligand field of the Fe(II) ion in the LS and HS states, and the (b) ball-and-stick model of the 3D Hofmann-like spin-crossover porous coordination polymer {Fe(pz)[Pt(CN)$_4$]}, where pz = pyrazine. Atom codes: Fe (orange); N (blue); C (green); Pt (gray); H (white).

would be quite crucial as the effects of interfacial interactions, on the device properties of a material, cannot be emphasised enough.[46–49]

Experimental details

The nanocrystals of 3D Hoffman-like {Fe(pz)[Pt(CN)$_4$]} were prepared using a synthesis procedure described in the literature.[50–52] The procedure consists of the preparation of a K_2[Pt(CN)$_4$] solution in water with constant stirring followed by a subsequent addition of a stoichiometric Fe(BF$_4$)$_2$·6H$_2$O and pyrazine solution in MeOH/H$_2$O (1 : 1). The precipitate was separated by centrifugation, washed with ethanol, and then dried under air at ambient temperature. The product {Fe(pz)[Pt(CN)$_4$]}·2H$_2$O was dehydrated at 400 K for more than 2 h under reduced pressure ($<10^{-2}$ Pa) to produce yellow, anhydrous, microcrystalline solids of {Fe(pz)[Pt(CN)$_4$]}.

The temperature-dependent variation of the spin-state occupancy in {Fe(pz)[Pt(CN)$_4$]} nanocrystals was probed through temperature dependent XPS measurements. These measurements were performed in a SPECS GmbH system (base pressure 1.0×10^{-10} mbar) equipped with a PHOIBOS 150 2D-CMOS hemispherical analyzer. Photoelectrons were excited with the Al-Kα line (1486.7 eV) of a monochromatic X-ray source µ-FOCUS 500 (SPECS GmbH) and the pass-energy for these measurements was set at 20 eV.

Results and discussion

The temperature-dependent photoemission spectra of the Fe 2p and N 1s core levels of {Fe(pz)[Pt(CN)$_4$]} collected over a range of temperature are shown in Fig. 2a and b, respectively. As described elsewhere,[6] the ligand-to-metal charge transfer (LMCT) will get weaker, due to the elongation of Fe–N bonds, as the temperature is increased; therefore, as before,[6] the HS electronic configuration is assigned in the XPS peak at the higher binding energy, whereas the LS electronic configuration is assigned in the XPS peak at the lower binding energy. This assignment of the XPS peaks is also consistent with the elevated effective nuclear charge experienced by the Fe 2p electrons in the HS configuration.[12,30–40] Based on the peak ratios of the fitted N 1s core-level components in Fig. 2b, it is clear that the N 1s features with greater peak areas and lower binding energies (N1) correspond to the nitrogen atoms in "Pt(CN)$_4$", whereas the N 1s features observed at higher binding energies (N2) correspond to the nitrogen atoms in "pyrazine". As can be seen from Fig. 2b, there are no discernible changes in the binding energy of either of the N 1s core-level components of our microporous coordination SCO complex, indicating that the HS electronic configuration of {Fe(pz)[Pt(CN)$_4$]} is quite stable.

The quantification of high-spin state occupancy in these systems is achieved by extracting the LS and HS peak areas from the temperature dependent XPS of the Fe 2p core-level of these materials (Fig. 2a) and then plotting the high-spin fractions of these molecules as a function of temperature, as shown in Fig. 3. Upon comparing the temperature dependence of the high-spin fractions of {Fe(pz)[Pt(CN)$_4$]} extrapolated from the XPS measurements (solid black and hollow blue triangles) with the temperature dependence of the ones obtained from the magnetic susceptibility measurements[53] (red curve), an apparent difference between the two kinds of measurements, stemming from the fact that XPS is a highly surface-sensitive technique (with penetration depths less than 10 nm [42,43]), is observed. Such a disagreement between the results obtained from the two kinds of measurement techniques is not something contradictory, because it simply implies that the surface of this material is different from its bulk, which is to be expected since usually the coordination number of the atomic species at the surface is significantly different from that of the atomic species in the bulk. In other words, as a highly likely possibility, the pronounced difference between the results of the abovementioned measurements elucidates that the HS tends to stabilize at the surface of {Fe(pz)[Pt(CN)$_4$]} not only at room temperature but also at temperatures well below the transition temperature for the whole molecule. Correlating with a lack of noticeable temperature-dependent shift in the binding energy of both the N 1s core-level components of this material (refer to Fig. 2b), as mentioned above, this fact can be attributed to the reasonable difference between the coordination numbers of the molecules at the surface of {Fe(pz)[Pt(CN)$_4$]} and those in its bulk. Such a difference between the coordination numbers of the molecules at the surface and the bulk of {Fe(pz)[Pt(CN)$_4$]} can potentially lead to the steric inhibition of the Fe(II) coordination environment,[54,55] and manifest itself as the analogous difference between the Ising-like antiferromagnetic superexchange
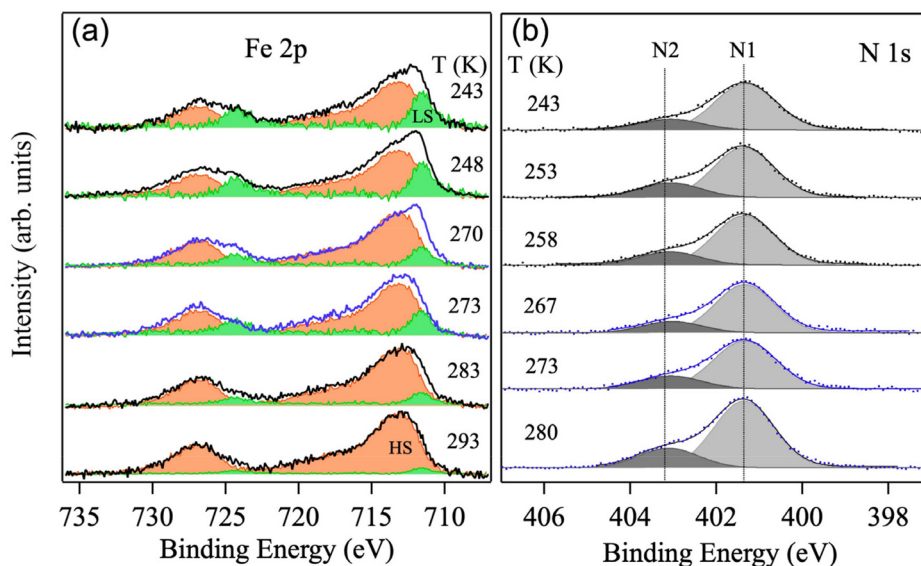
Fig. 2 Temperature-dependent photoemission spectra of the (a) Fe 2p and (b) N 1s core levels of {Fe(pz)[Pt(CN)$_4$]}. The raw spectra in blue depict lowering of temperature while the ones in black represent the increase in temperature. The fits in green indicate the LS, and the fits in orange represent the HS.
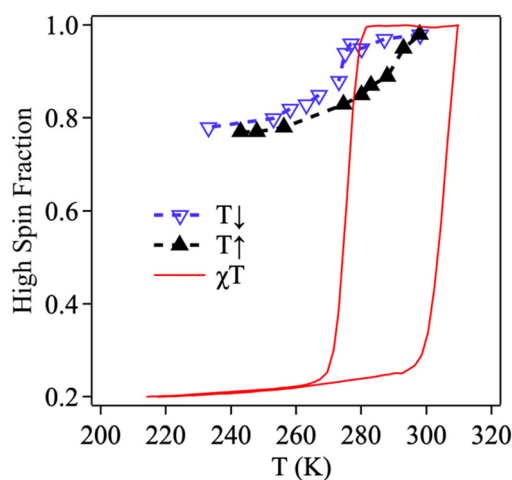

Fig. 3 Normalised high-spin fraction of {Fe(pz)[Pt(CN)$_4$]}, extrapolated from XPS (solid black and hollow blue triangles) and magnetic susceptibility measurements (red curve), as a function of temperature. The red curve, showing the magnetic susceptibility data, is extracted from ref. 53 and is included here to draw a comparison with the results of our XPS measurements.

interaction Hamiltonian (generally given as $J \sum_{k} m_{i,k}m_{i,k+1}$)[56] of its surface and bulk, respectively.

the existing literature, temperature-driven variations in the Fe 2p core-level spectrum of {Fe(pz)[Pt(CN)$_4$]} clearly evidence the expected spin-state transition in this 3D SCO system. Furthermore, the absence of detectable temperature-dependent shifts in the binding energies of the two N 1s core-level components (*i.e.*, the nitrogen atoms in "Pt(CN)$_4$" and the nitrogen atoms in "pz"), among quite a few possibilities, may indicate that the HS electronic configuration of this molecule can fend off thermal fluctuations. Even though, regardless of the choice of the measurement technique, the nanocrystals of {Fe(pz)[Pt(CN)$_4$]} are found to be in the high-spin state at temperatures in the vicinity of 300 K, drawing a direct comparison between the high-spin fractions extrapolated from the temperature-dependent XPS and the magnetic susceptibility measurements requires special attention due to steric inhibition effects. Therefore, the high value of room-temperature HS occupancy especially at the surface of the {Fe(pz)[Pt(CN)$_4$]} nanocrystal, and its great immunity to thermal fluctuations, opens new pathways for room-temperature spintronics and quantum information science applications. Overall, our results elucidate that the use of XPS to study the differences between the surface and bulk magnetic character of SCO materials is not limited just to a certain kind of SCO complex,[6] but it can rather be employed to investigate the aforementioned nature of a wide range of SCO complexes.

Conclusions

In summary, further physical insights into the spin-state transitions of the 3D Hofmann-like spin-crossover porous coordination polymer {Fe(pz)[Pt(CN)$_4$]} are obtained by employing temperature-dependent XPS measurements. In agreement with

Author contributions

JFSR conceived the idea and coordinated this work. JAR supervised the sample preparation and structural implications of photoemission results. AMS performed photoemission measurements and MCA, AD, and JFSR analysed and inter-

preted the experimental results. AD, MCA, and JFSR co-wrote the manuscript, with inputs from all authors. All authors have given approval to the final version of the manuscript.

Conflicts of interest

The authors declare that they have no known competing financial interests or personal relationships that could have appeared to influence the work reported in this paper.

Acknowledgements

References

1 M. Salimi, S. Fathizadeh and S. Behnia, *Phys. Scr.*, 2022, **97**, 055005.

2 X. Zhang, P. S. Costa, J. Hooper, D. P. Miller, A. T. N'Diaye, S. Beniwal, X. Jiang, Y. Yin, P. Rosa, L. Routaboul, M. Gonidec, L. Poggini, P. Braunstein, B. Doudin, X. Xu, A. Enders, E. Zurek and P. A. Dowben, *Adv. Mater.*, 2017, **29**, 1702257.

3 S. Rohlf, M. Gruber, B. M. Flöser, J. Grunwald, S. Jarausch, F. Diekmann, M. Kalläne, T. Jasper-Toennies, A. Buchholz, W. Plass, R. Berndt, F. Tuczek and K. Rossnagel, *J. Phys. Chem. Lett.*, 2018, **9**, 1491–1496.

4 G. Hao, A. Mosey, X. Jiang, A. J. Yost, K. R. Sapkota, G. T. Wang, X. Zhang, J. Zhang, A. T. N'Diaye, R. Cheng, X. Xu and P. A. Dowben, *Appl. Phys. Lett.*, 2019, **114**, 032901.

5 J. A. Real, A. B. Gaspar and M. C. Muñoz, *Dalton Trans.*, 2005, 2062.

6 A. M. Serra, A. Dhingra, M. C. Asensio, J. A. Real and J. F. S. Royo, *Phys. Chem. Chem. Phys.*, 2023, **25**, 14736–14741.

7 M. Sorai and S. Seki, *J. Phys. Chem. Solids*, 1974, **35**, 555–570.

8 H. A. Goodwin, *Coord. Chem. Rev.*, 1976, **18**, 293–325.

9 M. Reiher, *Inorg. Chem.*, 2002, **41**, 6928–6935.

10 V. Martínez, I. Boldog, A. B. Gaspar, V. Ksenofontov, A. Bhattacharjee, P. Gütlich and J. A. Real, *Chem. Mater.*, 2010, **22**, 4271–4281.

11 M. C. Muñoz and J. A. Real, *Coord. Chem. Rev.*, 2011, **255**, 2068–2093.

12 M. Gruber, T. Miyamachi, V. Davesne, M. Bowen, S. Boukari, W. Wulfhekel, M. Alouani and E. Beaurepaire, *J. Chem. Phys.*, 2017, **146**, 092312.

13 N. A. A. M. Amin, S. M. Said, M. F. M. Salleh, A. M. Afifi, N. M. J. N. Ibrahim, M. M. I. M. Hasnan, M. Tahir and N. Z. I. Hashim, *Inorg. Chim. Acta*, 2023, **544**, 121168.

14 T. Granier, B. Gallois, J. Gaultier, J. A. Real and J. Zarembowitch, *Inorg. Chem.*, 1993, **32**, 5305–5312.

15 P. Gütlich, in *Metal Complexes*, Springer Berlin Heidelberg, Berlin, Heidelberg, 2007, pp. 83–195.

16 G. Bradley, V. McKee, S. M. Nelson and J. Nelson, *J. Chem. Soc., Dalton Trans.*, 1978, 522–526.

17 Y. Zhang, *J. Chem. Phys.*, 2019, **151**, 134701.

18 T. K. Ekanayaka, K. P. Maity, B. Doudin and P. A. Dowben, *Nanomaterials*, 2022, **12**, 1742.

19 E. König and K. Madeja, *Chem. Commun.*, 1966, 61–62.

20 X. Jiang, G. Hao, X. Wang, A. Mosey, X. Zhang, L. Yu, A. J. Yost, X. Zhang, A. D. DiChiara, A. T. N'Diaye, X. Cheng, J. Zhang, R. Cheng, X. Xu and P. A. Dowben, *J. Phys.: Condens. Matter*, 2019, **31**, 315401.

21 A. Mosey, A. S. Dale, G. Hao, A. N'Diaye, P. A. Dowben and R. Cheng, *J. Phys. Chem. Lett.*, 2020, **11**, 8231–8237.

22 T. K. Ekanayaka, G. Hao, A. Mosey, A. S. Dale, X. Jiang, A. J. Yost, K. R. Sapkota, G. T. Wang, J. Zhang, A. T. N'Diaye, A. Marshall, R. Cheng, A. Naeemi, X. Xu and P. A. Dowben, *Magnetochemistry*, 2021, **7**, 37.

23 K. S. Kumar and M. Ruben, *Angew. Chem., Int. Ed.*, 2021, **60**, 7502–7521.

24 F. J. Valverde-Muñoz, A. B. Gaspar, S. I. Shylin, V. Ksenofontov and J. A. Real, *Inorg. Chem.*, 2015, **54**, 7906–7914.

25 Y. Zhang, *J. Chem. Phys.*, 2020, **153**, 134704.

26 G. Hao, A. S. Dale, A. T. N'Diaye, R. V. Chopdekar, R. J. Koch, X. Jiang, C. Mellinger, J. Zhang, R. Cheng, X. Xu and P. A. Dowben, *J. Phys.: Condens. Matter*, 2022, **34**, 295201.

27 A. Dhingra, X. Hu, M. F. Borunda, J. F. Johnson, C. Binek, J. Bird, A. T. N'Diaye, J.-P. Sutter, E. Delahaye, E. D. Switzer, E. del Barco, T. S. Rahman and P. A. Dowben, *J. Phys.: Condens. Matter*, 2022, **34**, 441501.

28 S. Bhatti, R. Sbiaa, A. Hirohata, H. Ohno, S. Fukami and S. N. Piramanayagam, *Mater. Today*, 2017, **20**, 530–548.

29 K. S. Murray, in *Spin-Crossover Materials*, John Wiley & Sons Ltd, Oxford, UK, 2013, pp. 1–54.

30 K. Burger, C. Furlani and G. Mattogno, *J. Electron Spectrosc. Relat. Phenom.*, 1980, **21**, 249–256.

31 K. Burger, H. Ebel and K. Madeja, *J. Electron Spectrosc. Relat. Phenom.*, 1982, **28**, 115–121.

32 T. K. Ekanayaka, H. Kurz, K. A. McElveen, G. Hao, E. Mishra, A. T. N'Diaye, R. Y. Lai, B. Weber and P. A. Dowben, *Phys. Chem. Chem. Phys.*, 2022, **24**, 883–894.

33 A. Pronschinske, R. C. Bruce, G. Lewis, Y. Chen, A. Calzolari, M. Buongiorno-Nardelli, D. A. Shultz, W. You and D. B. Dougherty, *Chem. Commun.*, 2013, **49**, 10446.

34 J.-Y. Son, K. Takubo, D. Asakura, J. W. Quilty, T. Mizokawa, A. Nakamoto and N. Kojima, *J. Phys. Soc. Jpn.*, 2007, **76**, 084703.

35 L. Poggini, G. Londi, M. Milek, A. Naim, V. Lanzilotto, B. Cortigiani, F. Bondino, E. Magnano, E. Otero, P. Sainctavit, M.-A. Arrio, A. Juhin, M. Marchivie, M. M. Khusniyarov, F. Totti, P. Rosa and M. Mannini, *Nanoscale*, 2019, **11**, 20006–20014.

36 L. Li, S. M. Neville, A. R. Craze, J. K. Clegg, N. F. Sciortino, K. S. A. Arachchige, O. Mustonen, C. E. Marjo, C. R. McRae, C. J. Kepert, L. F. Lindoy, J. R. Aldrich-Wright and F. Li, *ACS Omega*, 2017, **2**, 3349–3353.

37 E. C. Ellingsworth, B. Turner and G. Szulczewski, *RSC Adv.*, 2013, **3**, 3745.

38 A. P. Grosvenor, B. A. Kobe, M. C. Biesinger and N. S. McIntyre, *Surf. Interface Anal.*, 2004, **36**, 1564–1574.

39 A. R. Craze, C. E. Marjo and F. Li, *Dalton Trans.*, 2022, **51**, 428–441.

40 G. Agustí, R. Ohtani, K. Yoneda, A. B. Gaspar, M. Ohba, J. F. Sánchez-Royo, M. C. Muñoz, S. Kitagawa and J. A. Real, *Angew. Chem.*, 2009, **121**, 9106–9109.

41 T. K. Ekanayaka, H. Kurz, A. S. Dale, G. Hao, A. Mosey, E. Mishra, A. T. N'Diaye, R. Cheng, B. Weber and P. A. Dowben, *Mater. Adv.*, 2021, **2**, 760–768.

42 J. B. Gilbert, M. F. Rubner and R. E. Cohen, *Proc. Natl. Acad. Sci. U. S. A.*, 2013, **110**, 6651–6656.

43 S. D. Gardner, C. S. K. Singamsetty, G. L. Booth, G.-R. He and C. U. Pittman, *Carbon*, 1995, **33**, 587–595.

44 J. R. Galán-Mascarós, E. Coronado, A. Forment-Aliaga, M. Monrabal-Capilla, E. Pinilla-Cienfuegos and M. Ceolin, *Inorg. Chem.*, 2010, **49**, 5706–5714.

45 R. Torres-Cavanillas, M. Morant-Giner, G. Escorcia-Ariza, J. Dugay, J. Canet-Ferrer, S. Tatay, S. Cardona-Serra, M. Giménez-Marqués, M. Galbiati, A. Forment-Aliaga and E. Coronado, *Nat. Chem.*, 2021, **13**, 1101–1109.

46 A. Dhingra, D. Sando, P.-S. Lu, Z. G. Marzouk, V. Nagarajan and P. A. Dowben, *J. Appl. Phys.*, 2021, **130**, 025304.

47 Y. Bai, X. Meng and S. Yang, *Adv. Energy Mater.*, 2018, **8**, 1701883.

48 H. Zhang, Y. Li, X. Zhang, Y. Zhang and H. Zhou, *Mater. Chem. Front.*, 2020, **4**, 2863–2880.

49 A. Dhingra, D. E. Nikonov, A. Lipatov, A. Sinitskii and P. A. Dowben, *J. Mater. Res.*, 2023, **38**, 52–68.

50 V. Niel, J. M. Martinez-Agudo, M. C. Muñoz, A. B. Gaspar and J. A. Real, *Inorg. Chem.*, 2001, **40**, 3838–3839.

51 M. Ohba, K. Yoneda, G. Agustí, M. C. Muñoz, A. B. Gaspar, J. A. Real, M. Yamasaki, H. Ando, Y. Nakao, S. Sakaki and S. Kitagawa, *Angew. Chem., Int. Ed.*, 2009, **48**, 4767–4771.

52 D. Alvarado-Alvarado, J. H. González-Estefan, J. G. Flores, J. R. Álvarez, J. Aguilar-Pliego, A. Islas-Jácome, G. Chastanet, E. González-Zamora, H. A. Lara-García, B. Alcántar-Vázquez, M. Gonidec and I. A. Ibarra, *Organometallics*, 2020, **39**, 949–955.

53 G. Levchenko, A. B. Gaspar, G. Bukin, L. Berezhnaya and J. A. Real, *Inorg. Chem.*, 2018, **57**, 8458–8464.

54 J. M. Holland, S. A. Barrett, C. A. Kilner and M. A. Halcrow, *Inorg. Chem. Commun.*, 2002, **5**, 328–332.

55 A. R. Craze, M. M. Bhadbhade, Y. Komatsumaru, C. E. Marjo, S. Hayami and F. Li, *Inorg. Chem.*, 2020, **59**, 1274–1283.

56 H. Banerjee, S. Chakraborty and T. Saha-Dasgupta, *Inorganics*, 2017, **5**, 47.